RESEARCH ARTICLE

Mass and Heat Transfer in the Boundary Layer Region of Modified Second-Grade Fluid Flow Over a Linearly Stretched Sheet Embedded in Porous Media

N.G.A. Karunathilake and L.M.N.Fernando

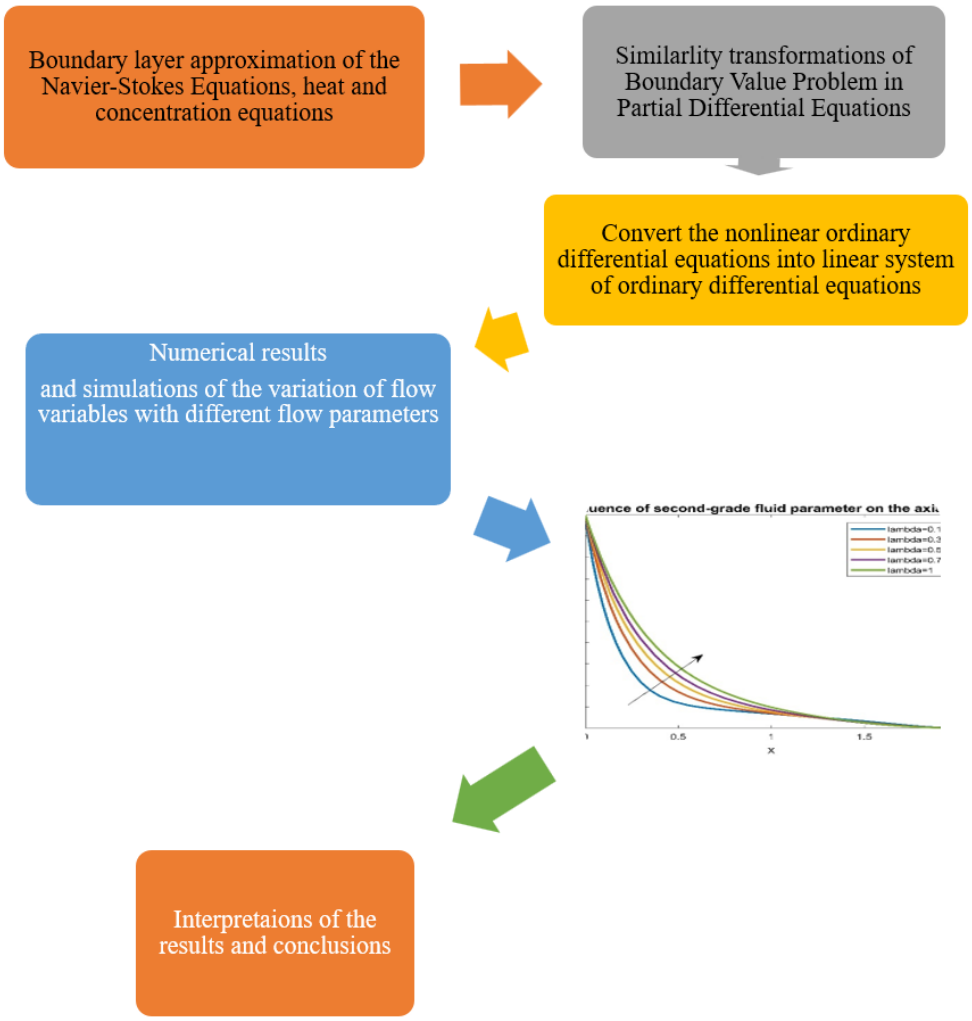

Highlights

- Boundary layer approximation of modified second-grade fluid flow can be successfully modelled.
- Fluid motion is enhanced by thermal and solutal Grashof number and second-grade fluid parameters.
- Magnetic, porous, and chemical reaction parameters suppress velocity, while they motivate temperature and concentration.
- Thermal and solutal Grashof numbers, second-grade fluid parameters, demotivate temperature and concentration,
- Flow variables of both shear-thickening and shear-thinning fluids behave similarly.

Ceylon Journal of Science 53 (2) 2024: 171-181
DOI: http://doi.org/10.4038/cjs.v53i2.8260

RESEARCH ARTICLE

Mass and Heat Transfer in the Boundary Layer Region of Modified Second-Grade Fluid Flow Over a Linearly Stretched Sheet Embedded in Porous Media

N.G.A. Karunathilake [1*], L.M.N.Fernando[1]

[1] *Department of Mathematics, University of Kelaniya, Kelaniya, Sri Lanka*

Received: 23.10.2023; Accepted: 24.02.2024

Abstract: Here, we have improved a model to describe the flow variables, velocity, mass and heat transfer in the boundary layer region of modified second-grade fluid flow over a linearly stretched sheet in a porous media. The modified model is used to study the qualitative impact of buoyancy parameter, second-grade fluid parameter, magnetic parameters, porous parameter, power-law index, and chemical reaction parameter on the flow profiles, radial and axial velocities, temperature, and concentration. Starting with the steady-state governing equations of mass, momentum, heat, and concentration of the fluid flow, we obtained the boundary layer approximations of the flow near the linearly stretched sheet with the no-slip boundary condition. Similarity transformation has been used to convert the partial differential equations system into a nonlinear ordinary differential equations system. The radial velocities, temperature, and concentration profiles have been solved numerically, and the qualitative influence of the flow parameters on the flow variables has been simulated and graphically presented for comparison. We have observed that radial and axial velocities were increasing for the shear-thinning and shear-thickening fluids with solutal Grashof number, thermal Grashof number and second-grade fluid parameters. In contrast, the porous and chemical reaction parameters slow down both fluids' radial and axial velocities. The temperature and concentration increase with the porous and magnetic parameters. However, thermal and solutal Grashof and second-grade fluid parameters suppress temperature and concentration. In shear-thickening fluids, chemical reaction parameters enhance concentration but suppress in shear-thinning fluids.

Keywords: Second-grade fluid, Shear-thinning, Shear thickening, Heat transfer, Porous media

INTRODUCTION

Many industrial processes widely use the boundary layer flow and heat and mass transfer of Newtonian and non-Newtonian fluids past a stretching sheet. Specifically, aerodynamics, food processing, chemical engineering, crystal growing, and polymer extrusion use heat and mass transfer methods. Compared to Newtonian fluids, non-Newtonian fluid is more in use in applications due to the viscosity variation and the complexity of the applications. Non-Newtonian fluids have a non-linear relation between viscosity and shear rate. However, in the absence of a unique relation between shear stress and viscosity in non-Newtonian fluids, various rheological models have been used to close the problem. The power law model, also known as the Ostwald de Waele model is one possible candidate. The model is much simpler than other non-Newtonian models and it assumes that the shear stress is propositional to some power of rate of strain and has only two fitting constants. In the power law model, there is a connoisseur description of the shear-thinning and shear-thickening behaviors of the fluids. The magnetohydrodynamic flow of an electrically conductive power-law fluid flow past a stretching sheet has been investigated by Andersson et al (Anderson et al. 1992). Their study considered the presence of a uniform transverse magnetic field. The power law model has been used by Andersson et al. (1996) to describe the unsteady fluid flow of a thin liquid film over a stretching surface. They used similarity transformation to reduce the non-linear boundary layer equations to a non-linear ordinary differential equation. One drawback of the power law model is that it cannot capture the normal stress behavior of some fluid flows, especially in shallow and very high shear rate regions. To address the issue, some researchers propose to combine the power law model with the second-grade fluid model, and the resulting model is known as the generalized (or modified) second-grade model. Aksoy et al. (2007) studied the two-dimensional incompressible fluid flow in the boundary layer region of a stretched sheet by using the modified second-grade non-Newtonian fluid model (Aksoy, 2007). In their research work, Lie Group theory has been used to calculate the boundary layer equations and the effects of the power-law index and second-grade coefficient on the boundary layers have been observed. They have shown that solutions are contrasted with the usual second-grade fluid solutions. The thermodynamic behavior and boundary layer flow of viscous incompressible fluid over a solid surface moving

**Corresponding Author's Email: gamage@kln.ac.lk*
https://orcid.org/0000-0001-8321-3615

continuously with constant speed has been studied by Sakiadis et al. (1961). Furthermore, the same authors discussed the numerical and integral methods to describe the incompressible, two-dimensional boundary layer flow on a continuous plane with constant speed in a fluid medium at rest (Hayat et al. 2017). Erikson et al. (1966) modified the work by considering heat and mass transfer in boundary layer flow. The author uses a moving surface with a non-zero transverse velocity. The heat transfer properties of a fluid flow over a stretching sheet were theoretically investigated by Carragher and Crane (Carraagher et al., 1982). Gupta & Gupta (1977) discussed momentum, heat, and mass transfer in the boundary layer flow past a stretching sheet under the effect of suction and blowing. Heat and mass transfer properties of a viscoelastic, electrically conducting, and viscous incompressible fluid over a vertical porous plate were studied by Nayak et al. (2014), who analyzed the effect of heat and mass transfer processes on the natural convection flow. Furthermore, Nayak et al. (2016) extended the study numerically by considering a stretching sheet in a porous medium under a magnetic field and chemical reaction effects. Hayat et al. (2017) recently studied the three-dimensional magnetohydrodynamic second-grade nanofluid flow past an exponentially stretching sheet under convective boundary conditions. Moreover, Hayat et al. (2016) studied the ferromagnetic second-grade fluid flow over a stretching sheet under the influence of viscous dissipation and magnetic dipole effects.

Very little attention has been given to the heat and mass transfer analysis of chemically reacting modified second-grade fluid over a linearly stretching sheet through a porous medium subjected to a magnetic field with a homogeneous first-order chemical reaction. Thus, this research study focuses on developing a mathematical model considering all effects, as mentioned earlier, and qualitative results can be utilized in many industrial processes.

Mathematical Formulations

A steady-state, incompressible, two-dimensional flow of a modified second-grade fluid flow over a linearly stretching sheet in a porous media is studied. The X-axis of the Cartesian coordinate-system runs parallel to the horizontal sheet, and the Y-axis is perpendicular to the sheet. The flow of the fluid is restricted to the plane y > 0. The stretching of the sheet along the X-axis generates fluid flow. The chemical reaction is assumed to occur uniformly everywhere within the fluid. The flow is considered to be over a linearly stretching sheet on the plane y = 0 with a porous medium. Figure 1 illustrates the physical configuration of the fluid flow domain with the necessary conditions.

Navier Stokes equation, Heat equation, Concentration equation, Ohm's law, and Maxwell's equations are starting governing equations and are given below.

$$\nabla.V = 0 \tag{1}$$

$$\frac{\rho DV}{Dt} = \nabla.\tau + J \times B - \frac{\nu u}{k_1} + g\beta_T(T - T_\infty) + g\beta_C(C - C_\infty) \tag{2}$$

$$J = \sigma\,(E + V \times B) \tag{3}$$

$$\nabla.B = 0 \tag{4}$$

$$\nabla \times B = \mu_m J, \qquad \nabla \times E = -\frac{\partial B}{\partial t}, \tag{5}$$

where V is the velocity of the fluid, J is the current density, B is the total magnetic field, β_T and β_C are the buoyancy parameters, T is the dimensional temperature, C is the dimensional concentration of the fluid, T_∞ and C_∞ represents the temperature and concentration of the ambient fluid.

Here, $B = B_0 + b$ with B_0 as the imposed magnetic field and b as the induced magnetic field. It is assumed that b is negligible compared to B_0. Since no electric field is present in the fluid flow region, from Ohm's law (3), the current density J = σ ($V \times B$). The Cauchy stress tensor for the modified second-grade fluid is given by,

$$\tau = -pI + \mu\pi^{\frac{m}{2}}A_1 + \alpha_1 A_2 + \alpha_2 A_1^2\ , \tag{6}$$

where p is the pressure, μ is the dynamic coefficient of viscosity, m is the power-law index, α_1 and α_2 are the normal stress coefficients and $\pi = \frac{1}{2}tr(A_1)^2$

$$A_1 = \nabla.V + (\nabla.V)^{\mathrm{T}} \tag{7a}$$

$$A_2 = \frac{dA_1}{dt} + A_1(\nabla V) + (\nabla V)^T A_1 \tag{7b}$$

This study assumes that the second-grade fluid model obeys the Clausius-Duhem inequality and is compatible with the fundamental Helmholtz free energy assumption.

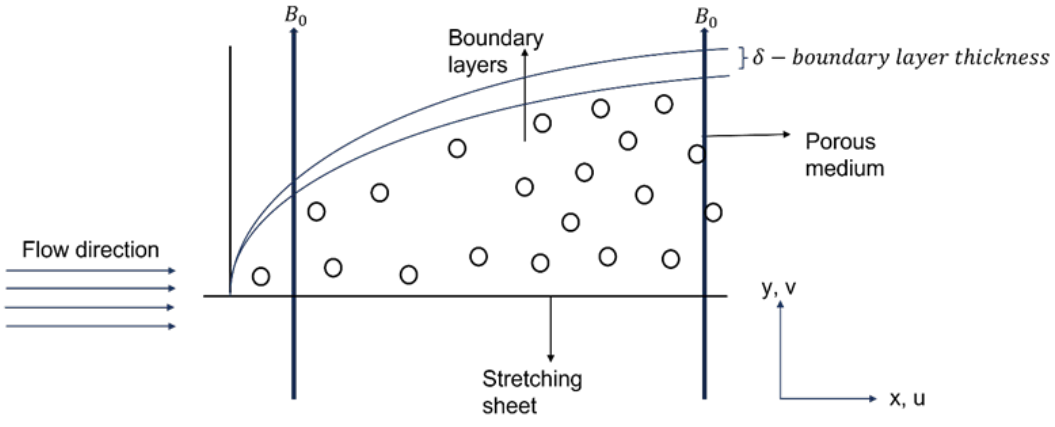

Figure 1: Flow Domain

Heat and mass concentration equations are given by.

$$u\frac{\partial T}{\partial x}+v\frac{\partial T}{\partial y}=\frac{k}{\rho C_p}\frac{\partial^2 T}{\partial y^2}+\frac{\mu}{\rho C_p}\left(\frac{\partial u}{\partial y}\right)^2+\frac{\lambda_1}{C_p}\frac{\partial u}{\partial y}\left[\frac{\partial}{\partial y}\left(u\frac{\partial u}{\partial x}+v\frac{\partial u}{\partial y}\right)\right]+\frac{Q}{\rho C_p}(T-T_\infty)+\frac{\sigma B_0^2}{\rho C_p}u^2 \quad (8)$$

$$u\frac{\partial C}{\partial x}+v\frac{\partial C}{\partial y}=D\frac{\partial^2 C}{\partial y^2}-k_2(C-C_\infty) \quad (9)$$

Here, $\lambda_1=\frac{\alpha_1}{\rho}, \nu=\frac{\mu}{\rho}, C_p$ is the specific heat capacity at constant pressure and T is the dimensional temperature, C is the dimensional concentration and D is the Brownian diffusion coefficient.

Boundary conditions are given by

$$u=ax, v=0, T=T_w-T_\infty+\frac{Ax^2}{l} \text{ and } C=C_w \text{ at } y=0$$

$$u\to 0, \frac{\partial u}{\partial y}\to 0, T\to T_\infty, \text{and } C\to C_\infty \text{ as } y\to\infty.$$

A linear velocity profile has been selected for the horizontal velocity at the boundary as the the sheet is stretched linearly.

Boundary layer approximation (See [Oleinik et al., 1999]) of the equations (1), (2), (8), and (9) take the form.

$$\frac{\partial u}{\partial x}+\frac{\partial v}{\partial y}=0 \quad (10)$$

$$u\frac{\partial u}{\partial x}+v\frac{\partial u}{\partial y}=\nu(m+1)\left(\frac{1}{2}\left(\frac{\partial u}{\partial y}\right)^2\right)^{\frac{m}{2}}\frac{\partial^2 u}{\partial y^2}+\lambda_1\left(\frac{\partial v}{\partial y}\frac{\partial^2 u}{\partial y^2}+v\frac{\partial^3 u}{\partial y^3}+\frac{\partial}{\partial x}\left(u\frac{\partial^2 u}{\partial y^2}\right)\right)-\frac{\sigma B_0^2}{\rho}u-\frac{\nu u}{k_1}+\frac{g\beta_T}{\rho}(T-T_\infty)+\frac{g\beta_C}{\rho}(C-C_\infty) \quad (11)$$

$$u\frac{\partial T}{\partial x}+v\frac{\partial T}{\partial y}=\frac{k}{\rho C_p}\frac{\partial^2 T}{\partial y^2}+\frac{\mu}{\rho C_p}\left(\frac{\partial u}{\partial y}\right)^2+\frac{\lambda_1}{C_p}\frac{\partial u}{\partial y}\left[\frac{\partial}{\partial y}\left(u\frac{\partial u}{\partial x}+v\frac{\partial u}{\partial y}\right)\right]+\frac{Q}{\rho C_p}(T-T_\infty)+\frac{\sigma B_0^2}{\rho C_p}u^2 \quad (12)$$

$$u\frac{\partial C}{\partial x}+v\frac{\partial C}{\partial y}=D\frac{\partial^2 C}{\partial y^2}-k_2(C-C_\infty) \quad (13)$$

In the Blasius boundary layer approximation view, we propose the following non-dimensional similarity transformation to convert the above nonlinear partial differential equations into a system of nonlinear ordinary differential equations

$$\eta=\sqrt{\frac{a}{\nu}}y, u=axf'(\eta), v=-f(\eta)\sqrt{a\nu}, \theta(\eta)=\frac{(T-T_\infty)}{T_w-T_\infty}, \phi(\eta)=\frac{C-C_\infty}{C_w-C_\infty}$$

The corresponding system of ODE takes the form.

$$f'(\eta)^2-f(\eta)f''(\eta)=(m+1)f'''(\eta)\left(\frac{1}{2}\right)^{\frac{m}{2}}\left(axf''(\eta)\sqrt{\frac{a}{\nu}}\right)^m-\lambda\left(-2f'(\eta)f'''(\eta)+f(\eta)f^{iv}(\eta)+f''(\eta)^2\right)-Mf'(\eta)-Pf'(\eta)+Gr_T\theta(\eta)+Gr_C\phi(\eta) \quad (14)$$

$$\theta''(\eta)+Prf(\eta)\theta'(\eta)-\Pr(2f'(\eta)-\alpha)\,\theta(\eta)+PrEc\lambda f''(\eta)\left(f'(\eta)f''(\eta)-f(\eta)f'''(\eta)\right)+PrEc\left(f''^2(\eta)+Mf'^2(\eta)\right)=0 \quad (15)$$

$$\phi''(\eta)+Sc\left(f(\eta)\phi'(\eta)-Kr\phi(\eta)\right)=0 \quad (16)$$

The continuity equation is trivially satisfied by the above similarity transformation.

The dimensionless parameters are defined as follows.

$\lambda=\frac{\lambda_1 a}{\nu}$ – Second-grade fluid parameter, $M=\frac{\sigma B_0^2}{\rho a}$ – Magnetic field parameter, $Gr_T=\frac{g\beta_T(T_w-T_\infty)}{2a^2}$ - Thermal Grashof number, $Gr_c=\frac{g\beta_C(C_w-C_\infty)}{2a^2}$ – Solutal Grashof number, $P=\frac{\nu}{k_1 a}$ – Porous parameter, $Pr=\frac{\mu C_p}{k}$ – Prandtl number, $Ec=\frac{a^2 l^2}{AC_p}$ – Eckert number, $Kr=\frac{k_2}{a}$ – Chemical reaction parameter, and $Sc=\frac{\nu}{D}$ – Schmidt number.

The corresponding boundary conditions are transformed as follows.

At $\eta=0$

$$f(0)=0, f'(0)=1, \theta(0)=1, \phi(0)=1$$

As $\eta\to\infty$

$$f'(\infty)\to\infty, f''(\infty)\to 0, \theta(\infty)\to 0, \phi(\infty)\to 0$$

The non-linear ODEs (14), (15), and (16) are converted into a linear system of ODEs using the following transformations.

$$f_1=f, f_2=\frac{df_1}{d\eta}, f_3=\frac{df_2}{d\eta}, f_4=\frac{df_3}{d\eta}, f_5=\theta, f_6=\frac{df_5}{d\eta}, f_7=\phi, f_8=\frac{df_7}{d\eta}$$

Then the resulting linear system of ODE takes the form.

$$\frac{df_4}{d\eta}=\frac{1}{\lambda f_1}\left((m+1)f_4\left(\frac{1}{2}\right)^{\frac{m}{2}}(xf_3)^m+f_1f_3-f_2^2+\lambda(2f_2f_4-f_3)-Mf_2-Pf_2+Gr_Tf_5+Gr_Cf_7\right)$$

$$\frac{df_6}{d\eta}=-Prf_1f_7+\Pr(2f_2-\alpha)\,f_6-PrEc[f_3^2+\lambda f_3(f_2f_3-f_1f_4)+Mf_2^2]$$

$$\frac{df_8}{d\eta}=-Sc[f_1f_7-Krf_8] \quad (17)$$

And the corresponding boundary conditions are,

at $\eta=0$,

$f(0)=0, f_2(0)=1, f_5=1, f_7=1$

as $\eta\to\infty$

$f_2(\infty)\to 0, f_3(\infty)\to 0, f_5(\infty)\to 0, f_7(\infty)\to 0,$

RESULTS AND DISCUSSION

The Boundary Value Problem (17) is a two-point boundary value problem, and we have used bvp4c MATLAB solver to obtain the desired solutions. We compute the solution in the similarity variable interval [0*;* 2]. The impact of the flow parameters on the radial velocity, axial velocity, temperature and concentration has been analyzed and presented graphically for comparison.

Effect of Fluid Parameters on Flow Profiles of the Shear Thickening Fluid Flow

In this section, we exhibit the impact of the fluid parameter on radial and axial velocities, temperature, and concentration for shear-thickening fluids.

The thermal Grashoff number represents the relation between inertia force, buoyant force, and viscous force in the fluid flow region. Figure 2 describes the impact of the thermal Grashof parameter. It can be observed that both radial and axial velocity fields are increased with the increase of the thermal Grashof number, but in contrast, both the temperature and concentration decrease. Hence, the velocities are motivated by inertia and buoyant forces over viscous forces. However, inertia and buoyant forces demotivate the temperature and concentration.

The solutal Grashoff number represents the ratio between the species' buoyancy force to the viscous hydrodynamic force. Figure 3 depicts the impact of the solutal Grashof number. The solutal Grashof number enhances both radial and axial velocities, but the temperature and the concentration decrease. Hence, the species' buoyancy force motivates the fluid motion compared to the viscous force. However, it has a converse effect on the temperature and the concentration.

Figure 4 demonstrates the impact of the second-grade parameter on fluid flow variables. We observe that the second-grade fluid parameter enhances both radial and axial velocities, thereby thickening the boundary layer region but degenerates the temperature and the concentration. Hence, the parameter thickens the boundary layer. However, the impact on concentration is insignificant compared to the temperature.

The chemical parameter represents the rate of chemical reaction. The variations of the flow variables with the chemical parameter is demonstrated in Figure 5. The scrutiny of the figures reveals both radial and axial velocity profiles and concentration profiles decrease with increasing chemical parameter values. Hence, the motion of the fluid is decelerated and the chemical reactions lower mass concentration. However, the temperature increases with the increase of the thermal Grashof number. Therefore, the chemical reactions generate heat.

The porous parameter is the ratio of pore volume to its total fluid volume, and it describes the porosity of the fluid region. Variations of the flow variables with the porous parameter are plotted in Figure 6. It is found that both velocities are decreased with the increase of the porous parameter. Hence, the porosity decelerates the fluid motion. The temperature and concentration increase with the increase of the porous parameter. Thus, porosity enhances the temperature and the concentration. However, the effect is not so significant.

The magnetic parameter represents the strength of the magnetic field in the boundary layer region. The effect of the magnetic parameter is demonstrated in Figure 7. Both radial and axial velocities are decreased by increasing the magnetic parameter. Hence, the presence of strong magnetic deaccelerated the fluid motion. However, both temperature and concentration are enhanced by the presence of the magnetic field.

Impact of the flow parameters in shear-thinning fluids

The impact of the fluid parameters on the flow variables for shear-thinning fluids is illustrated in this section.

Figure 8 describes the impact of the thermal Grashof parameter. It can be observed that both radial and axial velocity fields are increased with the increase of the thermal Grashof number, but in contrast, both the temperature and concentration decrease. Hence, the velocities are motivated by inertia and buoyant forces over viscous forces and the temperature and concentration are demotivated, although the impact on the concentration is insignificant.

Figure 9 demonstrates the impact of the solutal Grashof number. The solutal Grashof number enhances both radial and axial velocities, but the temperature and the concentration decrease. Hence, the species' buoyancy force motivates the fluid motion compared to the viscous force. However, it has a converse effect on the temperature and the concentration. However, we can observe that the impact on the concentration is insignificant compared to the impact on the other flow profiles.

Figure 10 demonstrates the trends of second-grade parameters on the flow profiles. It can be inspected that both radial and axial velocities are inspired by the second-grade parameter and temperature, and the concentration of the fluid gets lowered for the increment of the second-grade parameter. Hence, the low viscosity enhances the fluid motion and compresses temperature and concentration. However, the impact of the second-grade parameter on the concentration is insignificant compared to the impact on the other flow variables.

The variations of the flow variables with the chemical parameter are visualized in Figure 11. The e figures reveal both radial and axial velocity profiles and concentration profiles decrease with increasing chemical parameter values. Hence, the motion of the fluid is decelerated, and the chemical reactions lower mass concentration. However, the temperature increases with the increase of the thermal Grashof number. Therefore, the chemical reactions generate heat. It can be noticed further that the impact of the parameter on the velocities and the temperature is insignificant compared to the impact on the concentration.

Variations of flow variables with the porous parameter are illustrated in Figure 12. From the figure, it is perceived that an increase in the value of the porous parameter, the velocities of the fluid in the boundary layer region are decreasing. Thus, porosity degenerates the fluid motion. However, we notice that the temperature and concentration

increase with the parameter increase. Hence, the presence of porosity boosts the temperature and concentration.

The impact of the magnetic parameter is demonstrated in Figure 13. It can be observed that an increase in the value of the magnetic parameter, the axial velocity of the fluid in the boundary layer region is decreasing. Thus, the magnetic field degenerates the axial velocity. However, we notice that the axial velocity, temperature and concentration increase with the parameter increase. Hence, the presence of porosity boosts radial velocity, temperature and concentration.

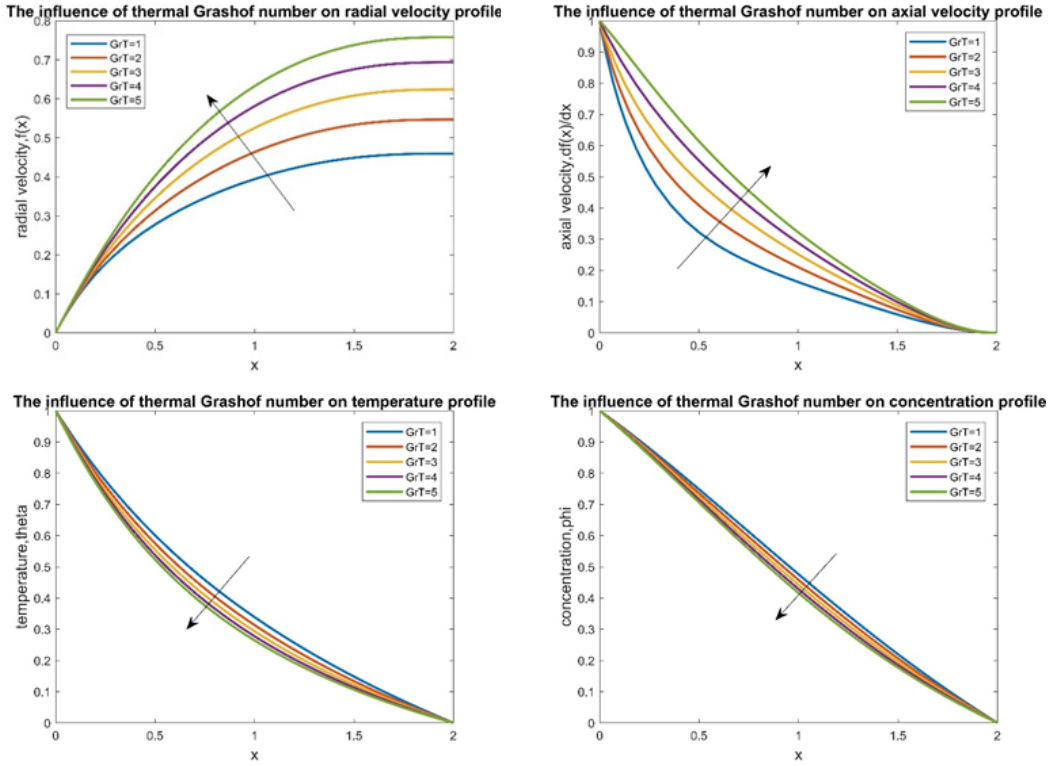

Figure 2: Impact of thermal Grashof number

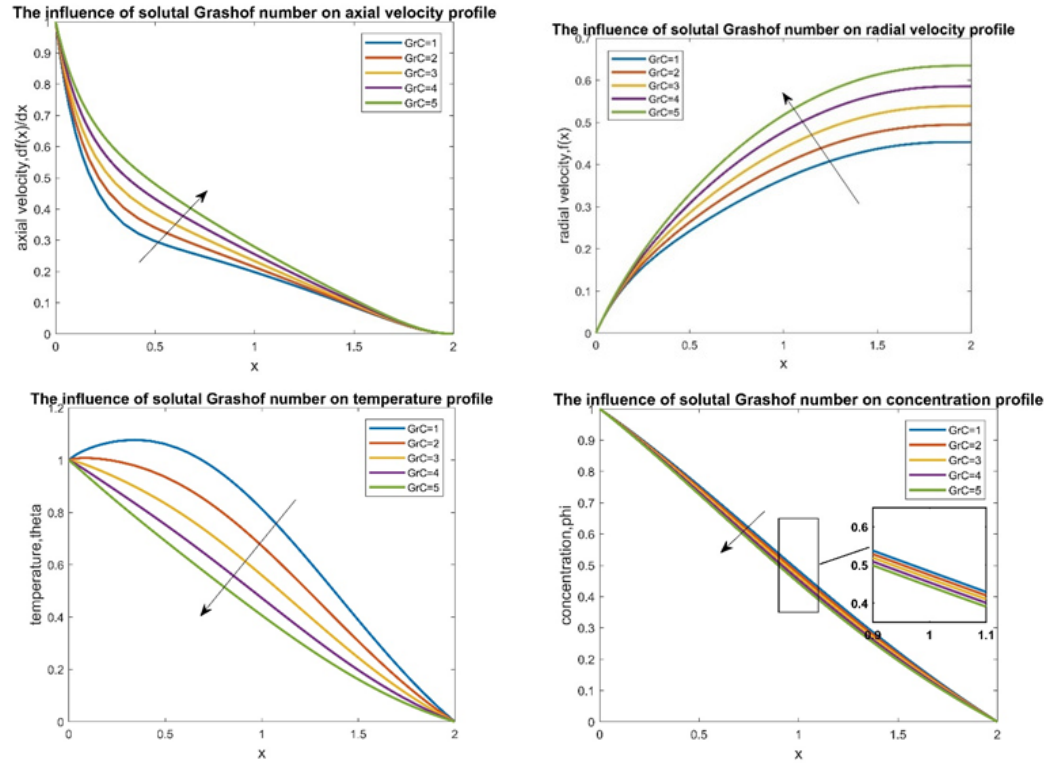

Figure 3: Impact of solutal Grashof number

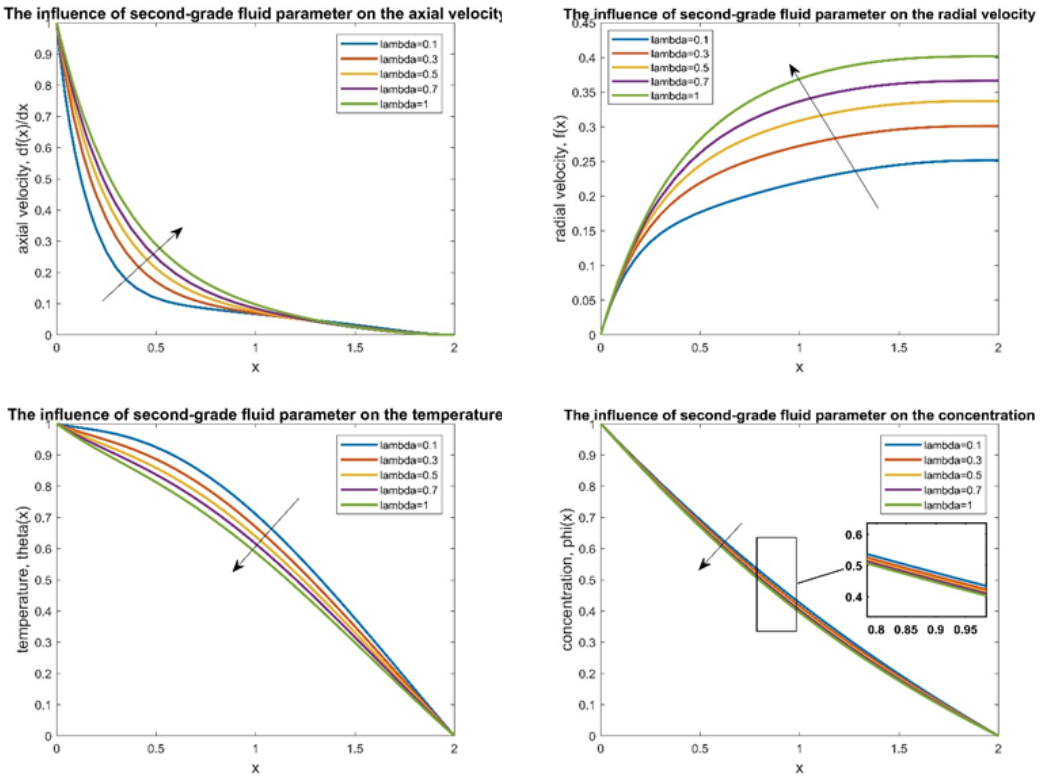

Figure 4: Impact of second-grade fluid parameter

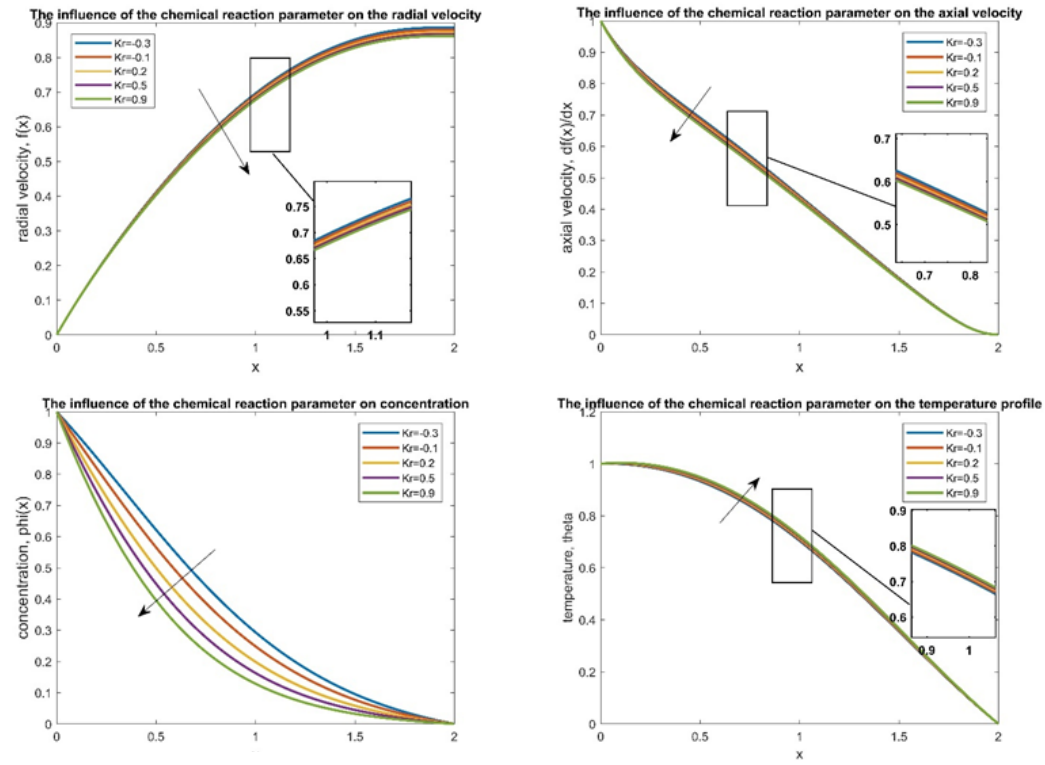

Figure 5: The impact of chemical reaction parameter

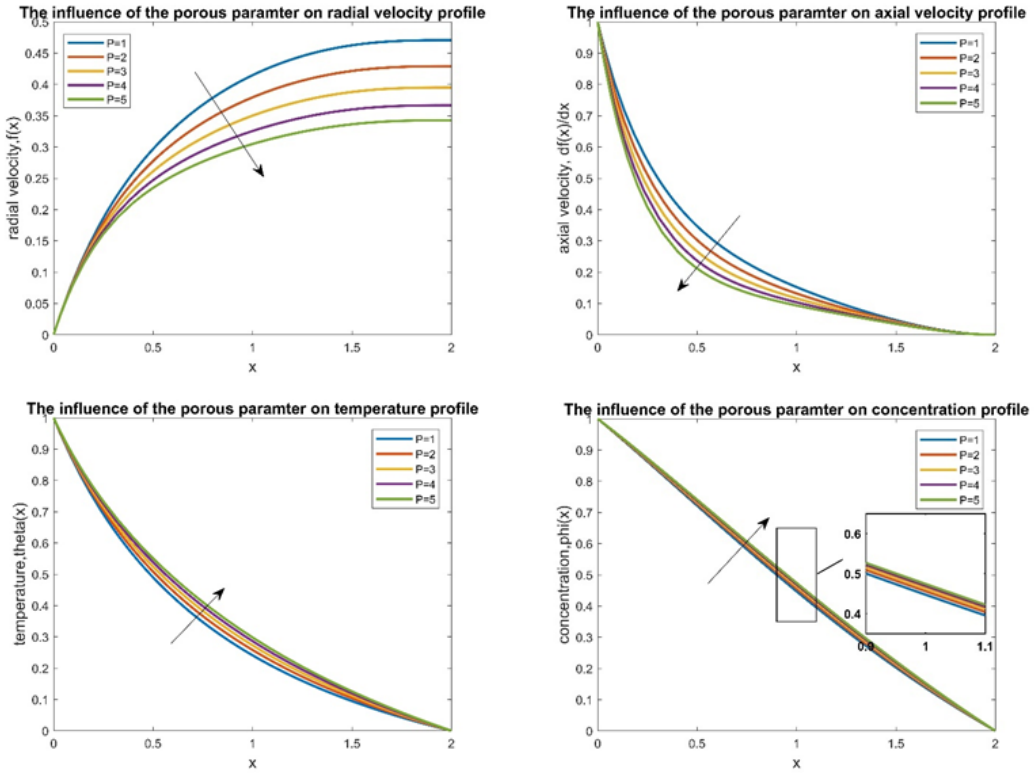

Figure 6: Impact of porous parameter

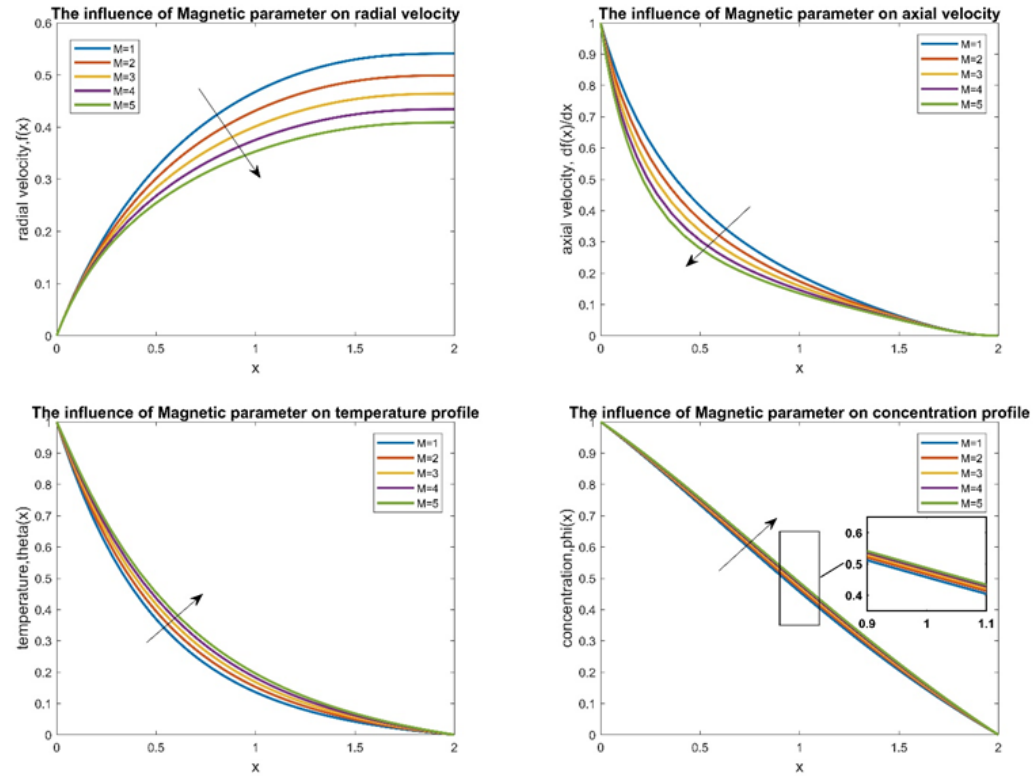

Figure 7: Impact of magnetic parameter

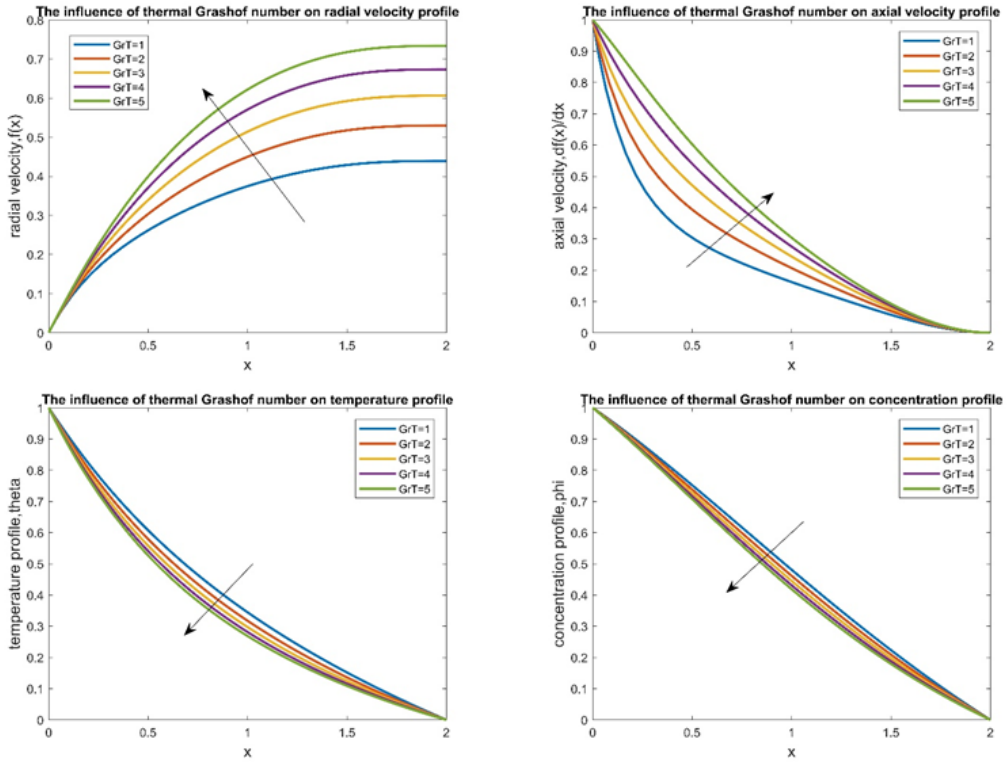

Figure 8: Impact of thermal Grashof number

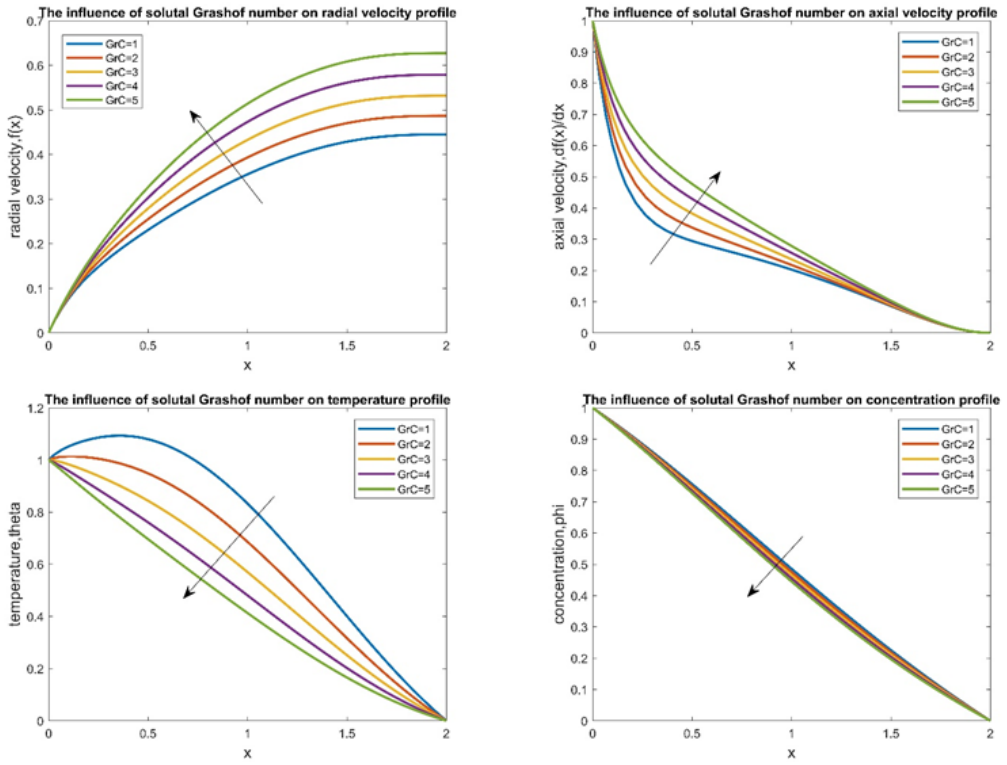

Figure 9: Impact of solutal Grashof number

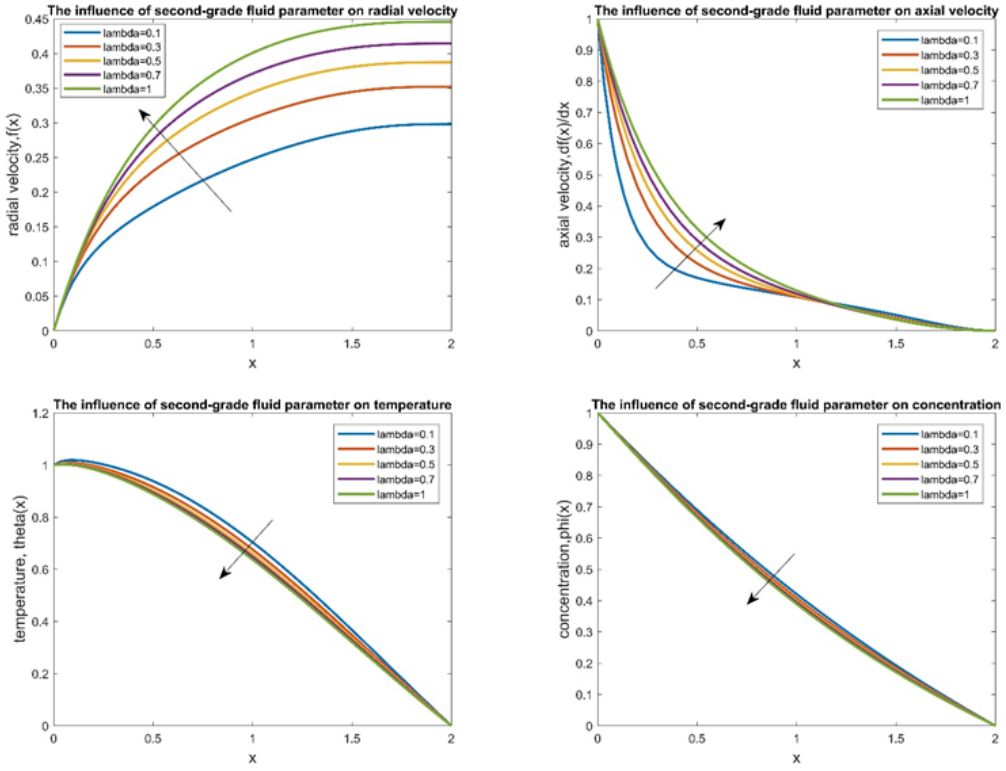

Figure10: Impact of second-grade fluid parameter

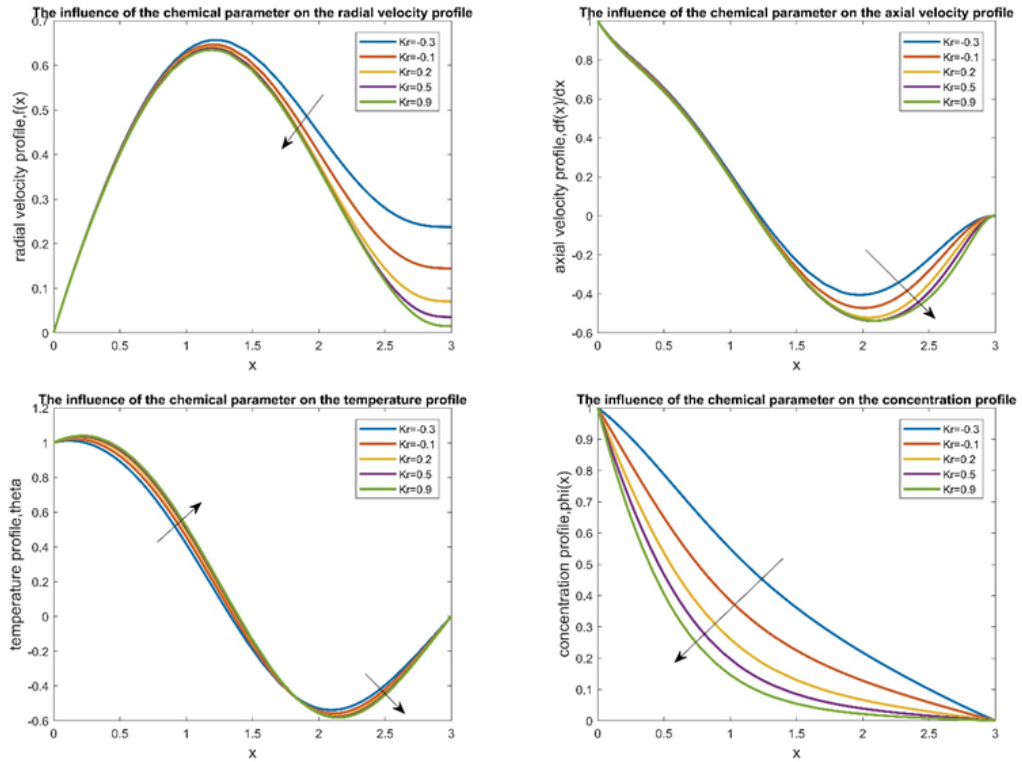

Figure 11: Impact of chemical reaction parameter

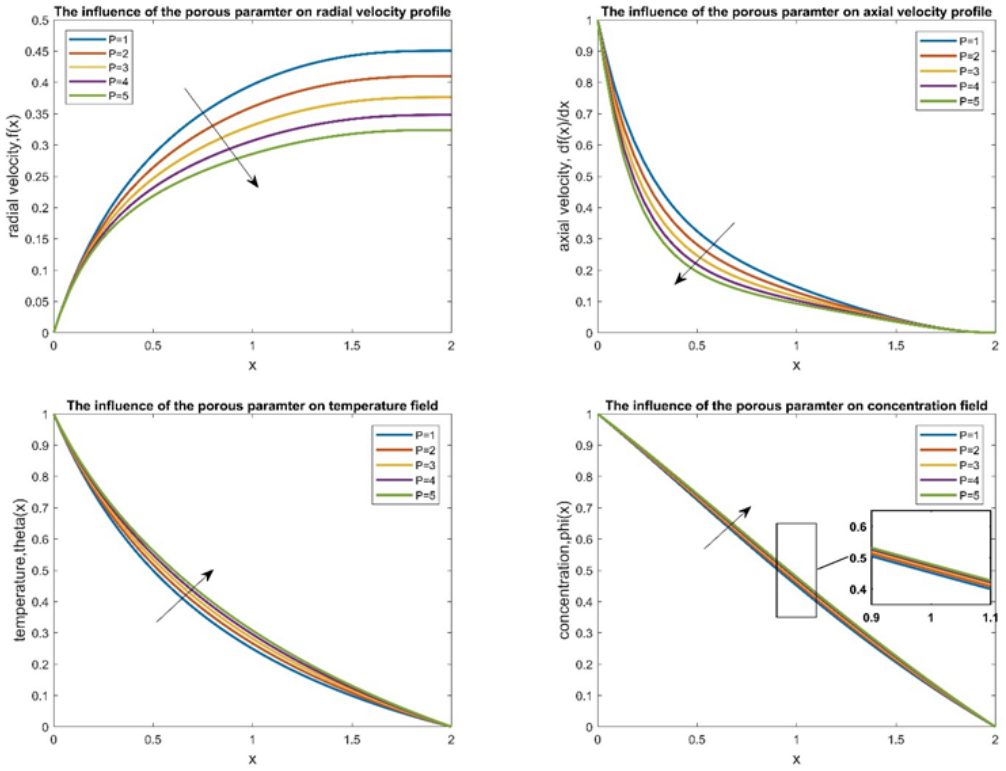

Figure 12: Impact of porous parameter

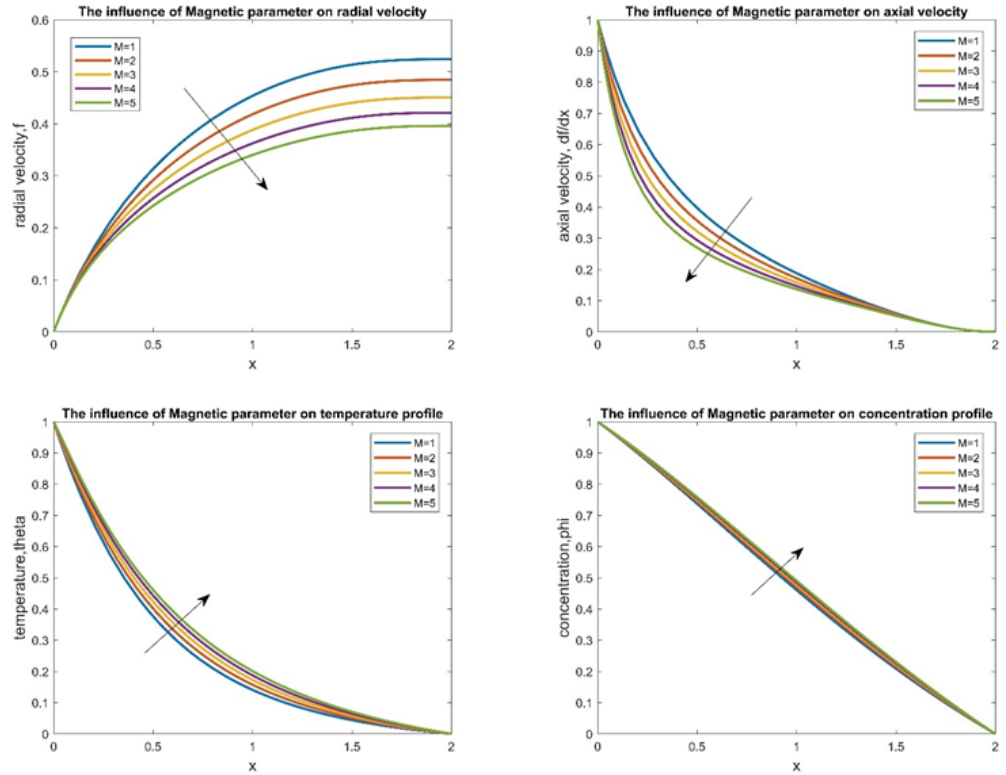

Figure 13: Impact of magnetic parameter

CONCLUSION

The following outcomes can be concluded from the analysis and the simulation results. For the shear-thickening fluids, both axial and radial velocity profiles are increasing for the increasing values of thermal and solutal Grashof number second-grade fluid parameter and are decreasing for the increasing values of the magnetic, porous, and chemical reaction parameters. Temperature profile is enhanced by the increasing values of chemical, porous and magnetic parameters and is demotivated by increasing values of thermal and solutal Grashof numbers, second-grade fluid parameter. Concentration profile is increasing for the increasing values of porous and magnetic parameters but is decreasing for the increasing values of thermal and solutal Grashof numbers and second-grade fluid and chemical parameters.

For the shear-thinning fluids, both axial and radial velocity profiles are increasing for the increasing values of thermal and solutal Grashof number second-grade fluid parameters and are decreasing for the increasing values of the porous and chemical reaction parameters. Axial velocity decreases with the increase of magnetic parameter, but the radial velocity increases. The temperature profile is enhanced by the increasing values of chemical, porous and magnetic parameters and is demotivated by increasing values of thermal and solutal Grashof numbers, second-grade fluid parameters. The concentration profile is increasing for the increasing values of porous and magnetic parameters but is decreasing for the increasing values of thermal and solutal Grashof numbers and second-grade fluid and chemical parameters.

CONFLICT OF INTEREST

The authors declare that there is no conflict of interest regarding the publishing the results of the study.

REFERENCES

Aksoy, Y., Pakdemirli, M., Khalique, C.M, (2007). Boundary layer equations and stretching sheet solutions for the modified second-grade fluid, *International Journal of Engineering Science*, **45**(10), 829–841. DOI:10.1016/j.ijengsci.2007.05.006

Andersson,H.I., Aarseth, J.B, Braud, N. & BS Dandapat, B.S. (1996). Flow of a power-law fluid film on an unsteady stretching surface. *Journal of Non-Newtonian Fluid Mechanics*,**62**(1), 1–8. https://doi.org/10.1016/0377-0257(95)01392-X

Andersson, H.I., Bech, K.H., & Dandapat, B.S. (1992). Magnetohydrodynamic flow of a power-law fluid over a stretching sheet. *International Journal of Non-Linear Mechanics*, **27**(6), 929-936. https://doi.org/10.1016/0020-7462(92)90045-9

Carragher,P. and LJ Crane, L. J. (1982). Heat transfer on a continuous stretching sheet. *Zeitschrift Angewandte Mathematik und Mechanik*, **62**(10), 564–565. https://doi.org/10.1002/zamm.19820621009

Erickson L, Fan L, Fox V. (1966). Heat and mass transfer on moving continuous flat plate with suction or injection. *Industrial & Engineering Chemistry Fundamentals*; **5**(1), 19–25. http://dx.doi.org/10.1021/i160017a004

Gupta P, Gupta A (1977). Heat and mass transfer on a stretching sheet with suction or blowing. *The Canadian journal of chemical engineering,* **55**(6): 744–746. https://doi.org/10.1002/cjce.5450550619

Hayat, T., Ullah I., Muhammad, T., Alsaedi A. (2016). Magnetohydrodynamic (MHD) three-dimensional flow of second grade nanofluid by a convectively heated exponentially stretching surface. *Journal of Molecular Liquid*, 220: 1004–1012. DOI:10.1016/j.molliq.2016.05.024

Hayat, T, Khan, M.I., Alsaedi, A., Waqas M. (2017). Mechanism of chemical aspect in ferromagnetic flow of second-grade liquid. *Results in Physics*, **7**,4162–4167. https://doi.org/10.1016/j.rinp.2017.10.021

Nayak M, Dash G, Singh, L. (2014). Effect of chemical reaction on MHD flow of a visco-elastic fluid through a porous medium. *Journal of Applied Analysis Computation* **4**(4), 367–381.DOI:10.1007/s11012-015-0329-3

Nayak, M.K., Dash, G.C. (2016). Singh LP. Heat and mass transfer effects on MHD viscoelastic fluid over a stretching sheet through porous medium in presence of chemical reaction. *Propulsion and Power Research*, **5**(1), 70–80. https://doi.org/10.1016/j.jppr.2016.01.006

Oleinik, O.A., Samokhin V. (1999). *Mathematical Models in Boundary Layer Theory*. Chapman and Hall/CRC. DOI: https://doi.org/10.1201/9780203749364

Sakiadis, B. (1961). Boundary-layer behavior on continuous solid surfaces: The boundary layer on a continuous flat surface. *AiChE journal,* 7(2), 221–225. http://dx.doi.org/10.1002/aic.690070211